Quality monitoring and bias correction of satellite data in JRA-25

S. Kobayashi[1], M. Sakamoto[1], K. Kato[2], and T. Matsumoto[1]

[1] *Japan Meteorological Agency, Japan*
[2] *Meteorological Satellite Center/Japan Meteorological Agency, Japan*

Abstract

Japan Meteorological Agency (JMA) and the Central Research Institute of Electric Power Industry (CRIEPI) are conducting Japanese 25-year Reanalysis (JRA-25). In advance to the JRA-25 production, precise quality monitoring for TIROS Operational Vertical Sounder (TOVS) data has been preformed. Orbital elements of NOAA satellites can be estimated from earth-location of TOVS data with reasonable accuracy, and effective in monitoring bad earth-location. Also calibration data are effective in quality monitoring. Classification of poor quality data and detecting methods are described.

Precipitation of the JRA-25 has the highest correlation with the independent precipitation estimates: the CPC Merged Analysis of Precipitation (CMAP) and Global Precipitation Climate Project (GPCP), among reanalyses. On the other hand, there are some discontinuities in temperature time series in the stratosphere, which are coincident with satellite switching. The quality of the JRA-25 product relevant to satellite data is discussed.

1. Introduction

JMA and CRIEPI are conducting JRA-25 -- a joint research project to make a long-term and high-quality, global atmospheric reanalysis dataset. The dataset is expected to be beneficial for various climate information services and researches. The reanalysis period of JRA-25 is 26 years from 1979 to 2004. Production of JRA-25 was started in April 2004 and about 83% of the period had been completed as of November 2005. The entire period will be completed by March 2006. After the completion of the production, JRA-25 system will be transitioned to the JMA operational Climate Data Analysis System (JCDAS). Some of basic JRA-25 reanalysis products are supplied to operational meteorological centres and researchers via the Internet (http://www.jreap.org/download/download-e.html).

The quality of the JRA-25 products depends both on the quality control of observational data and performance of assimilating system. TOVS radiances have never been used in the JMA operational numerical weather prediction (NWP) system. So we have developed a quality monitoring method and an assimilating scheme for TOVS radiances. Fortunately, information about the quality of the TOVS data can be obtained from some sources (e.g. Kidwell, 1998; Hernandez et al., 2004). Close examination into the TOVS data, however, revealed that there were many poor quality data, which were not recorded in the sources. Precise quality monitoring for the TOVS data was developed and performed in advance to the JRA-25 production.

Although an up-to-date data-assimilation system is used for reanalyses, there is difference in quality between reanalyses, which is considered to be due to difference in satellite data assimilation schemes. In particular, bias correction for satellite radiances is difficult. We examined quality of precipitation and stratospheric temperatures of JRA-25, which are considered to be sensitive to a bias correction scheme for satellite data.

This paper describes precise quality monitoring for TOVS data, assimilation schemes for TOVS, Advanced TOVS (ATOVS) and Special Sensor Microwave/Imager (SSM/I) data, and the quality of the JRA-25 product relevant to those satellite data.

2. Precise quality monitoring for TOVS data

The TOVS system consists of three separate and independent instruments, HIRS, MSU and Stratospheric Sounding Unit (SSU). The TOVS had been successively on board the series of NOAA polar orbiting meteorological satellites from TIROS-N to NOAA 14. The TOVS data are available from 1978, and cover the most of JRA-25 reanalysis years. The TOVS gives temperature profiles and water vapor content especially in the stratosphere and over the ocean where conventional observation network is sparse. Close examination into the dataset revealed some kinds of poor quality data.

2.1. Classification of poor quality data

a. Bad earth-location

Figure 1 (a) shows data over the Persian Gulf are shifted north along the satellite track. Brightness temperatures from the MSU channel 1 are plotted. This channel is sensitive to the surface emissivity. There is a clear contrast between the brightness temperatures over land and those over sea because the emissivity of land surface and that of sea surface are quite different in the microwave region. This channel is, therefore, useful to check bad earth-location. Figure 1 (b) shows that the data in the circle are straying into the wrong time. Figure 1 (c) shows miss-located data are scattered out of the satellite orbit.

b. Noisy data

Figure 1 (d) shows a striped pattern appears in a brightness temperature. This striped pattern often appears in plots of the HIRS channel 1-3. Figure 1 (e) shows an example of random noise.

c. Partial level down of brightness temperatures of the HIRS

Calibration of the HIRS instrument is performed once every 256 seconds (40 lines). Calibration is provided by viewing an internal target and space. Figure 1 (f) shows brightness temperatures in the calibration period all fell down. It has been reported that there are similar phenomena in Geostationary Meteorological Satellite (GMS) infrared images (Hirooka, 1983). This phenomenon occurs in the case that the instrument views the moon in calibration processes. The magnitude depends on both age and position of the moon.

d. Discontinuity of brightness temperatures at boundaries of a super swath of the HIRS

The phenomenon is significant in CO_2 4.3-micron channels (13-17) (shown in Fig. 1 (g)). For channel 16, brightness temperature variation at boundaries is 4 to 16 times larger than that of interior, depending on seasons and local time of measurements (shown in Fig. 2). The variation of PM satellites is larger than that of AM satellites, and gradually decreases with long-time drift in the local time of measurements. The variation of PM satellites reaches the peak in February, whereas that of AM satellites in June.

e. Deterioration of instruments

The quality information sources give periods of deterioration of instruments. Brightness temperature time series also help detect such periods.

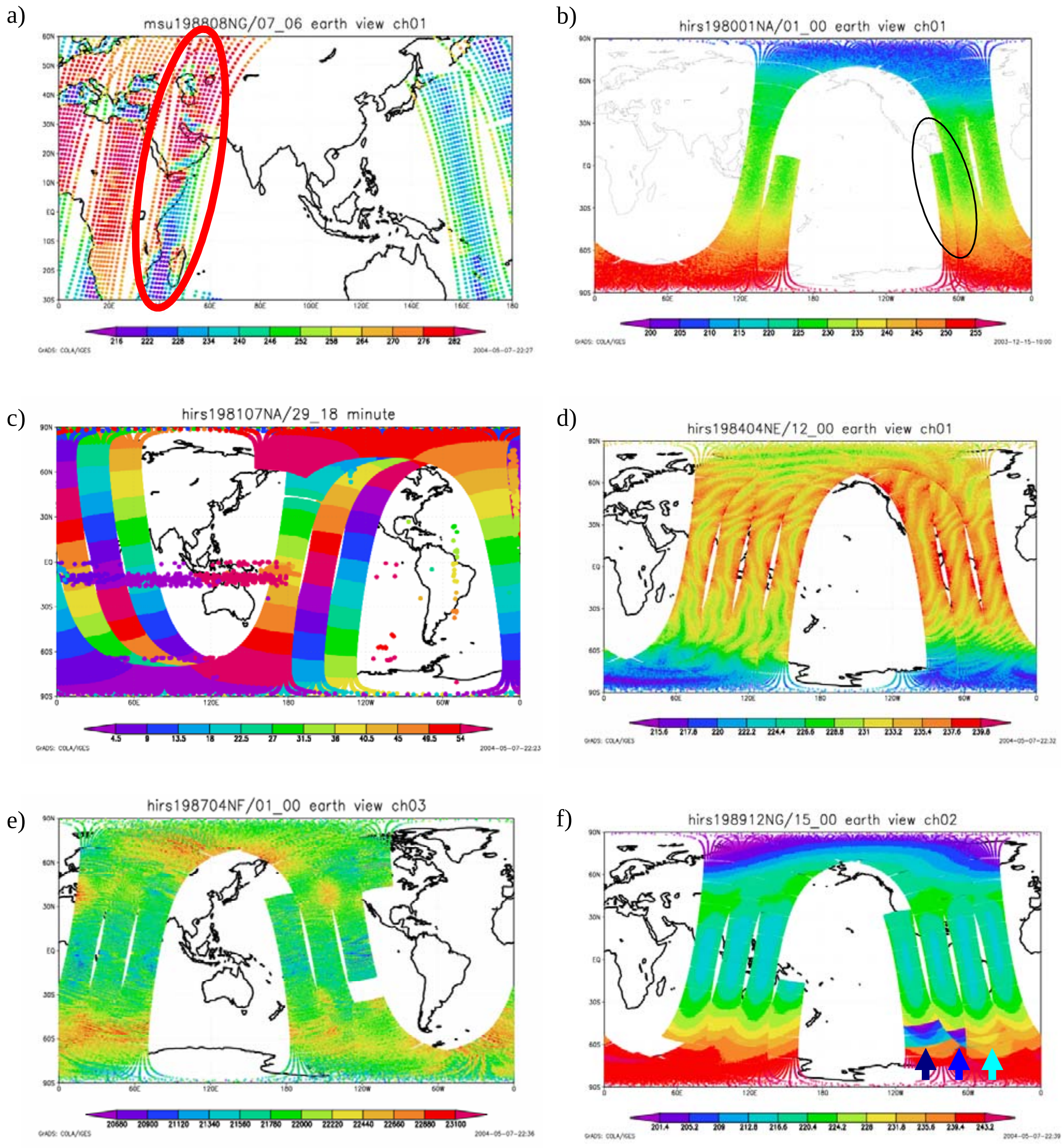

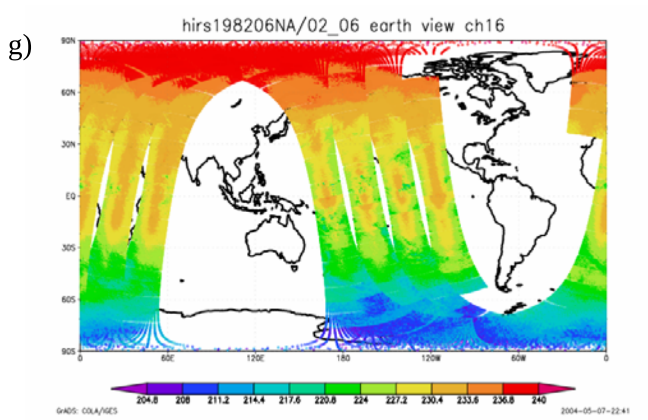

Figure 1 Typical examples of poor quality data of TOVS. (a), (b) and (c) show bad earth-location. (d) and (e) show noisy data. (f) shows partial level down of brightness temperatures of the HIRS. (g) shows discontinuity of brightness temperatures at boundaries of a super swath of the HIRS

2.2. Detecting methods for the poor quality data

Following methods were used to detect the poor quality data, and a detailed blacklist has been produced.

a. Bad earth-location

Firstly, distance between each couple of successive 20 data was calculated. In the case that the distance differed from a nominal value (Schwalb, 1978) over 120km, the couple of data were removed. Then, orbital elements were estimated from a couple of data in successive scan-lines, of which scan direction was the nearest to nadir. In the case that inclination or local time of ascending node differed from a nominal value (Schwalb 1978) over the pre-defined threshold, or position of satellites discontinuously changed (shown in Fig. 3), the period was blacklisted.

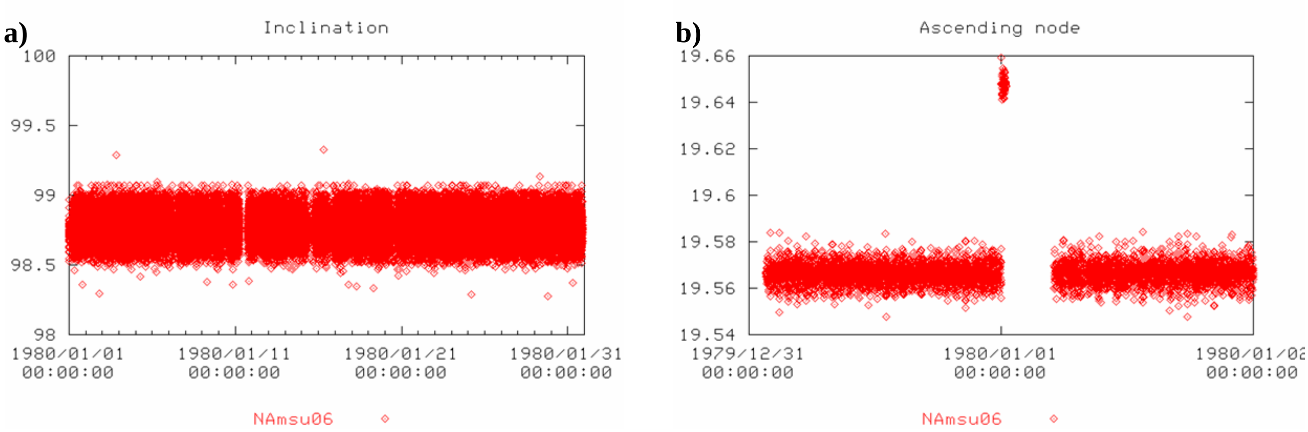

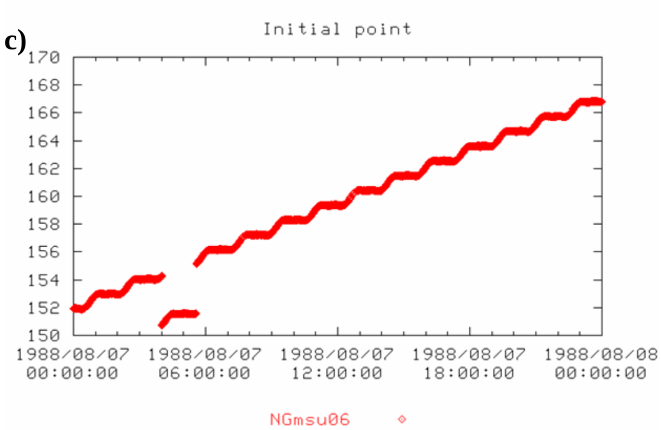

Figure 2 Orbital elements of NOAA spacecraft estimated from earth-location of TOVS data. (a) shows inclination. (b) shows local time of ascending node for the period corresponding to Fig. 1 (b). (c) shows direction angle of NOAA spacecraft from ascending node. The origin is the center of the earth. The period corresponds to Fig 1 (c)

b. Noisy data

Temperatures of an internal warm target (hereafter IWT), which is used for calibration of HIRS, are stable at 290K. It is considered that variance of radiances from IWT has correlation with magnitude of instrument noise. Time series of the variance were used to detect noisy data, and the periods were blacklisted (Fig. 4).

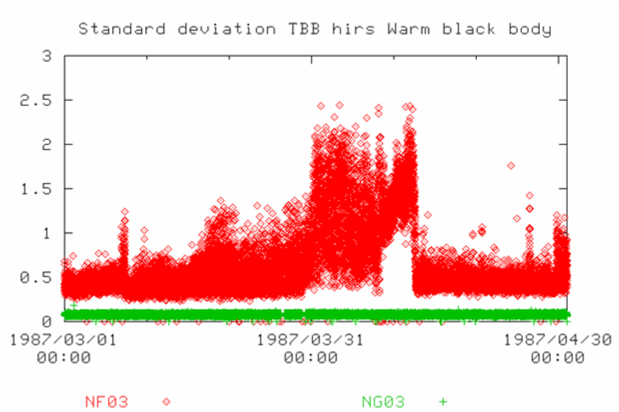

Figure 3 Standard deviation of brightness temperatures of the internal warm target. The red line shows HIRS channel 3 of NOAA 9, and the green line shows that of NOAA 10.

c. Partial level down of brightness temperatures of the HIRS

Apart from an IWT, there is an internal cold target (hereafter ICT) in the HIRS/2 instrument. Because of large temperature gradients induced by solar effects throughout the orbit, the ICT is not used for calibration of the HIRS. Therefore, brightness temperatures of the ICT can be used for validation of calibration. In the case that the instrument views the moon in calibration processes, increase in space view radiances is expected. Increase in space view radiances brings rise in intercept and fall in slope of calibration coefficients. Brightness temperatures derived with these coefficients are lower than real ones. The magnitude of decrease in brightness temperatures is comparable with spatial variation of brightness temperatures of earth view (shown in Fig. 5 (a)). On the other hand, it can be found easily in the brightness temperature time series for the ICT because the brightness temperatures of the ICT are rather stable between 260K and 270K (Fig. 5 (b)). Periods specified with the method were blacklisted.

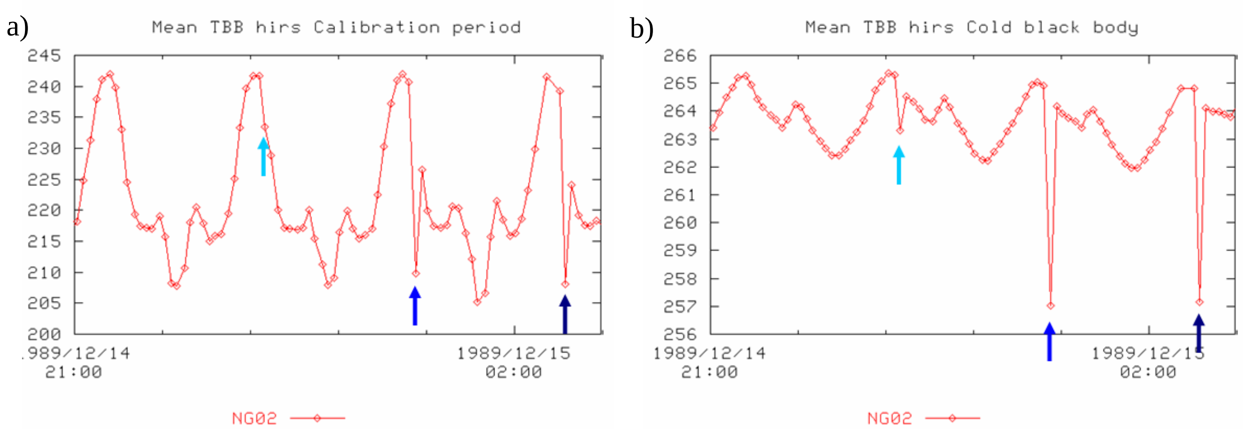

Figure 4 Calibration period average brightness temperatures for the period corresponding to Fig 1 (f). (a) shows earth-view, and (b) shows the internal cold target.

3. Assimilating schemes for TOVS, ATOVS and SSM/I data

3.1. TOVS

The assimilating scheme for TOVS radiances used in JRA-25 was developed on the bases of a former operational scheme for ATOVS level-1d data (Okamoto et al., 2005). RTTOV-6 (Saunders et al., 1999) is used for radiative transfer calculation. One-dimensional variational method (1DVAR) is performed as part of QC processes. In the case that the 1DVAR doesn’t converge well, the poor quality data are eliminated. To process HIRS and MSU data together in the 1DVAR, level-1d data were produced from level-1c data beforehand. To minimise bad influence of mapping, the nearest neighbor method was adopted (Sakamoto et al. 2005). Table 1 shows the channels used in JRA-25.

Clear, ice-free sea	HIRS ch2-7, 10-12, 15, MSU ch2-4, SSU ch1-3
Cloudy, ice-free sea	HIRS ch2,3, MSU ch4, SSU ch1-3
Sea-ice	HIRS ch2,3, MSU ch4, SSU ch1-3
Land	HIRS ch2,3, MSU ch4, SSU ch1-3

Table 1. Assimilated channels of TOVS in JRA-25.

Unlike operational NWP systems, it is impossible to estimate biases for each satellite and instrument in advance to reanalysis productions because of the enormous amount of data. It made us decide to use an adoptive bias correction scheme for TOVS data. In the scheme, optimum solutions of the 1DVAR are used as reference values. The bias correction coefficients are calculated from the latest 4-day sample dataset and revised every cycle. These coefficients are calculated for each 5K of observed brightness temperatures. This scheme is intended to correct inconsistency among channels in vertical one dimension, so difference between observations and background is not taken into account. Also coefficients for the SSU tend to be estimated smaller because SSU data are processed separately from the other sensors in the 1DVAR. Consequently, large-scale analysis increments occurred in stratospheric temperatures along satellite tracks, and the stratospheric temperatures were heaving up each cycle in a preliminary experiment. To reduce the oscillatory increments, time windows are expanded from 6 hours to 12 hours for stratospheric observing channels: channel 2 of the HIRS and all channels of the SSU, in JRA-25.

3.2. ATOVS

The assimilating scheme for ATOVS data in JRA-25 is the same as the operational scheme for direct assimilation of ATOVS level-1c data, which has been used in the JMA global analysis system since March 2005. This scheme is based on the former scheme for ATOVS level-1d data (Okamoto et al. 2005). RTTOV-7 is used for radiative transfer calculations. Table 2 shows the channels used in the JRA-25. HIRS is characterized by the small observation error, whereas its radiances are sensitive to clouds. This means that exact cloud detection is required. Such a cloud detection scheme for HIRS level-1c data has not been developed in the operational NWP system of JMA. On the other hand, AMSU radiances are less sensitive to clouds, which enables to make an observation under clouds unless the clouds don't include large particulates. Also the number of channels increased from 4 in the MSU to 20 in the AMSU. For these reasons, HIRS data are not used.

Clear or Cloudy, ice-free sea	AMSU-A channel 4-13, AMSU-B channel 3-5
Thick cloud, ice-free sea	AMSU-A channel 7-13, AMSU-B channel 3-5
Rainy, ice-free sea	AMSU-A channel 7-13
Sea-ice	AMSU-A channel 6-13
Land	AMSU-A channel 6-13

Table 2. Assimilated channels of ATOVS in JRA-25.

Two types of corrections are performed to correct biases of AMSU-A: One is for biases dependent upon scanning angles (hereafter scan bias), and the other is for biases dependent upon atmospheric conditions at observing spots (hereafter air-mass bias). The air-mass bias correction is a linear regression with the computed radiances from AMSU-A channels 5, 7 and 10, and surface temperatures as predictors. The regression coefficients are calculated from match-up dataset with radiosonde observations. With regard to AMSU-B, only the scan bias correction is applied. These coefficients were calculated from three-month sample dataset collected from June 2003 to August 2003, and applied throughout the period without being revised.

3.3. SSM/I

Total precipitable water (TPW) retrieved from microwave radiances has been used operationally in the JMA meso-scale analysis system. In the JRA-25, the same scheme is applied and TPW retrieved from SSM/I radiances are assimilated. The algorithm used in the scheme was developed in the Meteorological Satellite Center of JMA, and is applicable for no-scattering-affected radiances over sea (Takeuchi 2002). In the algorithm, 19, 22 and 37 GHz channels radiances are used with ancillary data such as surface temperatures, sea surface wind speed and temperatures at 850hPa.

Scan directions in the SSM/I from No. 51 to No. 64 are not used in the JMA meso-scale analysis system because SDRs processed by NESDIS are unsymmetricaly biased. The SDRs are also biased against the data decorded by NASA/Marshall Space Flight Center (MSFC) using Wents’s Decord-4 algorithm. To adjust the SDRs to MSFC data, bias correction for the SDRs is performed in the JMA meso-scale analysis system. In addition, bias correction for the retrieved TPW is also performed to adjust the TPW to that of the background. In the JRA-25, bias correction for TDRs supplied by NOAA/NESDIS and CLASS was performed to adjust the TDRs to MSFC data by using Wents’s Decord-4 algorithm. Bias correction for the retrieved TPW is performed as well, and the coefficients are constant throughout the period.

4. Quality of the JRA-25 product relevant to satellite observations

4.1. Precipitation

The correlation of JRA-25 global total precipitation and both CMAP and GPCP Ver. 2 observational precipitation datasets is the highest among the reanalysis. Figure 6 (a) shows the time series of the spatial correlation coefficients with CMAP for each reanalysis. The coefficient of the JRA-25 is high especially after July 1987 with assimilating SSM/I TPW retrievals. Figure 7 shows comparison of TPW increments between with and without SSM/I TPW retrievals. TPW decreased slightely and detailed distribution is given with TPW retrievals, while TPW increased slightly from background without the retrievals. Figure 6 (b) shows precipitation of JRA-25 is stable throughout the period, while the precipitation decreased slightly after July 1987. The good performance is believed to be owing to two reasons: The first is that the bias correction for TPW retrievals was performed to adjusted to those of background. The second is that the channels, of which radiances are sensitive to aerosols, were hardly used due to the strict clear-sky identification for the HIRS. In the time series of JRA-25, there is no significant increase in precipitation suffered by large-scale volcanic eruptions (El Chichon and Mt. Pinatubo) as found in ERA-40

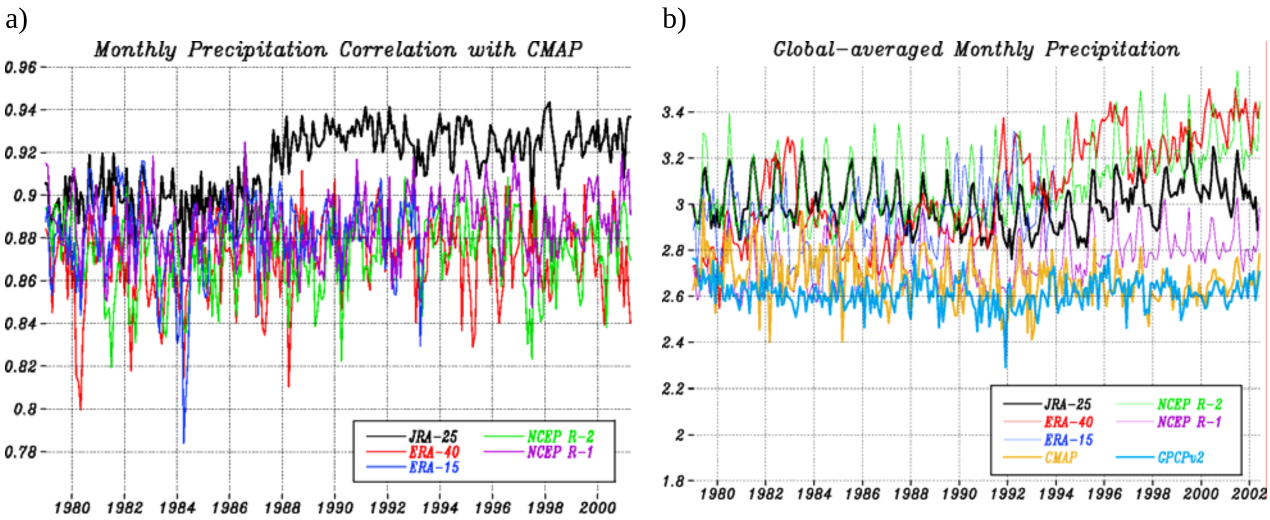

Figure 5 (a) shows correlation time series for monthly global mean precipitation with CMAP, and (b) shows global mean monthly precipitation time series

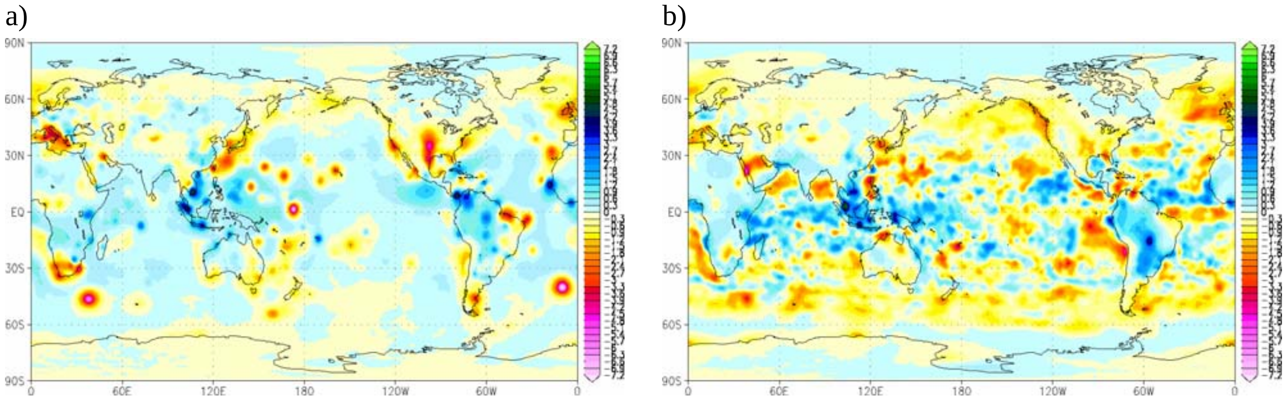

Figure 6 Monthly average increment of total column water vapor. (a) Dec 1983 (without SSM/I), (b) Dec 1991 (with SSM/I). Blues colors indicate moistening by the assimilation.

4.2. Stratospheric temperatures

Assimilation of stratospheric temperatures depends upon the data from strong absorption band channels of TOVS and ATOVS. Adjustments are required to compensate for radiometric and spectroscopic biases that are not taken into account by the radiative transfer model. It is, however, complicated because there are few independent observations that can be used as reference. Figure 8 shows time series of global mean temperature anomaly in the stratosphere for each reanalysis with the periods for which observations from each instrument and spacecraft are assimilated in JRA-25. All time series indicate warming after the large-scale volcanic eruptions (El Chichon and Mt. Pinatubo), and there is agreement on month-to-month variations. There is, however, significant difference in magnitude and trend of anomaly. Also there are some discontinuities that are coincident with satellite switching. In JRA-25, big jumps occurred from January to February 1995 while observations from the SSU were absent, and in October 1999 when the ATOVS replaced the TOVS. The discontinuities are more significant as altitude increases.

With regard to the SSU, which is a kind of the pressure-modulated CO_2 radiometer (PMR), it has been pointed out that there is necessity to take into account spectroscopic drifts due to the cell pressure changes (Brindley et al., 1999). The PMR employs a cell containing CO_2 as a filter. The pressure and hence transmission of this cell is periodically modulated, resulting in the selection of thermal radiation from the strong lines in the spectrum of atmospheric CO_2. This radiation originates in the 40-80-km region of the atmosphere. Assuming that absorption lines are strong, isolated and Lorentz shaped, an analytical expression for the peak pressure of the weighting function would be expected as follows (Taylor et al. 1972):

$$p_{peak} = \left[\frac{4(1+b)l}{a} \right]^{1/2} p_0$$

where p_0 is the mean pressure of the CO_2 cell, a is the total amount of CO_2 in the atmosphere (atm cm/atm), b is the self-broadening coefficient for CO_2, and l is the length of the CO_2 cell. Brindley et al. (1999) examined the effect of the CO_2 cell pressure changes of SSU channel 1 from TIROS-N to NOAA-11. The CO_2 cell pressure varied from 106.5 to 117.5 mb, while the nominal value is 100mb. The radiance variation due to the cell pressure changes is estimated from –0.15 to +0.13% (0% is corresponds to 111.5mb). However, the CO_2 cell pressure and the atmospheric CO_2 concentration are assumed to be constant throughout the period in JRA-25. The spectroscopic drift is not inclusive in the bias correction because the bias correction coefficients for the SSU are estimated smaller as mentioned earlier. It is, therefore, believed that the discontinuities in the stratospheric temperatures are partly because of the inappropriate spectroscopic parameters.

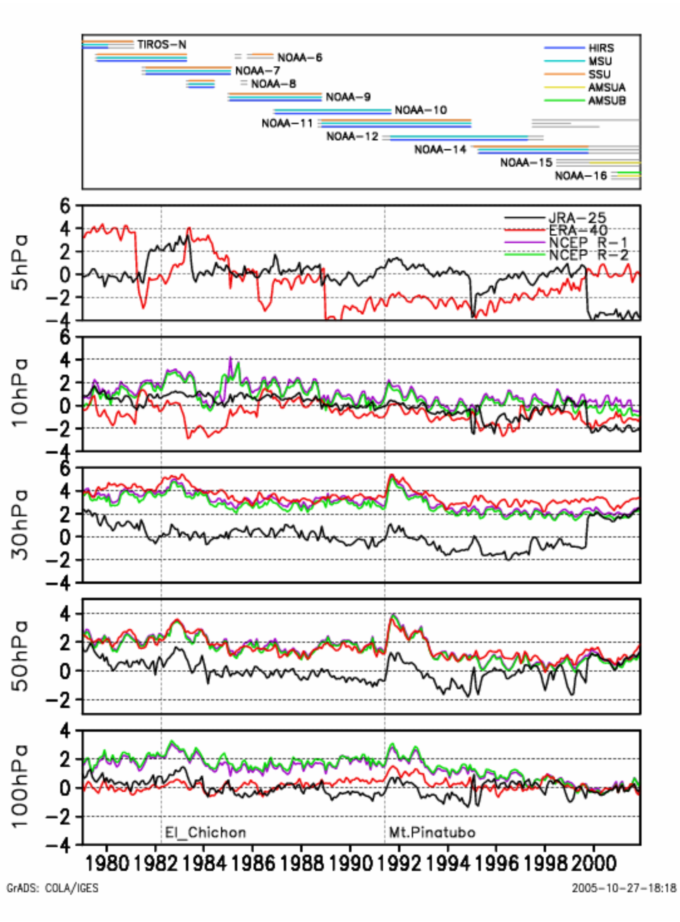

Figure 7 Global mean temperature anomaly time series for the stratosphere and the periods for which observations from each instrument and spacecraft are assimilated in JRA-25. The normal is calculated from the JRA-25 reanalysis from 1979 to 2000. The vertical dashed lines indicate the volcanic eruptions of El Chichon (1982) and Mt. Pinatubo (1991)

5. Conclusion

Precise quality monitoring for TOVS data has been performed by using estimated orbital elements and calibration data. Orbital elements of NOAA satellites can be estimated from earth-location of TOVS data with reasonable accuracy, and effective in monitoring bad earth-location. Also calibration data are effective in quality monitoring. These calibration data are, however, attached only to the HIRS of TOVS among the TOVS/ATOVS level-1c dataset supplied by ECMWF. So this method hasn't been applied to the other instruments. Although it turned out that there was discontinuity at the boundaries of super swath in HIRS CO_2 4.3 micron channels, we haven't come up to cope with it. These warrants further examination for level-1b data. Because all the information required for calibration are recorded on level-1b data, more precise quality monitoring would be possible. Also comparison with the latest calibration algorithm would provide information about radiometric biases.

Precipitation of the JRA-25 has the highest correlation with the independent precipitation estimates: CMAP and GPCP, among the reanalyses. It is believed to be due to the following two reasons; the first is that the bias correction for SSM/I data was performed to adjust to background TPW. The second is that strict QC is performed for water vapor channels of the HIRS. On the other hand, there are some discontinuities in temperature time series in the stratosphere, which are coincident with satellite switching. This means that bias correction is not appropriately performed for the stratospheric observing channels of TOVS and ATOVS. It is believed that these biases are partly because of inappropriate spectroscopic parameters assumed in the radiative transfer calculation (e.g. absorbing gas concentrations, CO_2 cell pressure of the SSU). For the HIRS and the MSU, Chedin et al. (2002) examined sensitivity to the change of the spectroscopic parameters. Similar examination for the SSU would provide quantitative estimates of the spectroscopic biases.

Acknowledgement

Most of conventional data including NCEP/NCAR observation and all the TOVS/ATOVS radiance data used in JRA-25 are supplied by ECMWF. SSM/I radiance data before 1997 were supplied by NCDC. SSM/I TPW retrievals are produced for JRA-25 in JMA. We appreciate very much for all the data supplier and producer to JRA-25. And also we appreciate to all researchers who gave us useful advices and suggestions.

References

Brindley, H. E., A. J. Geer, and J. E. Harries, 1999: Climate Variability and Trends in SSU Radiances: A Comparison of Model Predictions and Satellite Observations in the Middle Stratosphere, J. Climate, 12, 3197-3219.

Chedin, A., S. Serrar, R. Armante, N. A. Scott, and A. Hollingsworth, 2002: Signatures of Annual and Seasonal Variations of CO_2 and Other Greenhouse Gases from Comparisons between NOAA TOVS Observations and Radiation Model Simulations, J. Climate, 15, 95-116.

Hernandez, A., G. Kelly, and S. Uppala, 2004: The TOVS/ATOVS observing system in ERA-40. ERA-40 Project Rep. 16

Hirooka, G., 1983: Partial level down in brightness of Geostationary Meteorological Satellite (GMS) Infrared (IR) images caused by the moon, MSC Technical note, 8, 61-66.

Ishii, M., A. Shouji, S. Sugimoto and T. Matsumoto 2005: Objective Analyses of Sea-Surface Temperature and Marine Meteorological Variables for the 20th Century Using ICOADS and the KOBE Collection. Int. J. of Climatology, 25, 865-879.

Kidwell, K. B. (ed), 1998: NOAA Polar Orbiter Data User's Guide, November 1998 revision. Available on line from http://www2.ncdc.noaa.gov/docs/podug/.

Okamoto, K., M. Kazumori, and H. Owada 2005: The Assimilation of ATOVS Radiances in the JMA Global Analysis System. J. Meteor. Soc. Japan 83, 201-217.

Sakamoto, M., et. al. S. Kobayashi, K. Kato, T. Matsumoto, H. Koide, K. Onogi and T. Ose 2005: Ongoing Japanese Long-term Reanalysis Project (JRA-25); Assimilation of NOAA Polar-orbiter Satellite Sounder

Data. Proceeding of the 85th American Meteorological Society annual meeting, Ninth Symposium on Integrated Observing and Assimilation Systems for Atmosphere, Oceans, and Land Surface, Jan 8-14, 2005, P1.10.

Saunders, R.W., M. Matricardi and P. Brunel 1999: An improved fast radiative transfer model for assimilation of satellite radiance observations. Quart. J. R. Meteorol. Soc., 125, 1407-1425.

Schwalb, A., 1978: The TIROS-N/NOAA A-G satellite series. NOAA technical memorandum NESS 95.

Takeuchi, Y. 2002: Algorithm theoretical basis document(ATBD) of the algorithm to derive total water vapor content from ADEOS-II AMSR. EORC Bull, 9, 3-7.

Taylor, F. W., J. T. Houghton, G. D. Peskett, C. D. Rodgers, and E. J. Williamson, 1972: Radiometer for Remote Sounding of the Upper Atmosphere, Appl. Opt., 11, 135-141.